Revised submission to THREE 26th April 2018

Track structure and the quality factor for space radiation cancer risk.

Dudley T. Goodhead
Medical Research Council
Harwell, UK (Emeritus)

Abstract

A major risk from exposure to space radiation is the induction of cancer and it is from estimates of this risk that the maximum career flight times of NASA space crew members are restricted by a permissible exposure limit. For the purpose of demonstrating compliance with the career limit, NASA has developed a cancer risk projection model for exposure-induced fatal cancer, in which the formulation and numerical values of the quality factor (QF_{NASA}) are substantially different from those of the quality factor (Q) or radiation weighting factor (w_R) routinely applied for radiation protection on earth. The quality factor is used to account for the increased effectiveness of radiations of high linear energy transfer (LET), compared to the effectiveness of low-LET γ-rays derived from epidemiological studies of the atomic-bomb survivors. The need for a special approach for space radiation is dictated by the special characteristics of the charged particles from solar radiation and especially the charged particles of high energy and charge (HZE) in galactic cosmic rays (GCR). This article considers aspects of radiation track structure in relation to the relative biological effectiveness (RBE) of HZE particles and the quality factor used for space radiation. The NASA quality factor (QF_{NASA}) is composed of two terms, which can be interpreted as broadly representing the low- and the high-ionization-density components of the HZE particle tracks. These are discussed in turn as they relate to available experimental evidence on the biological effectiveness of such components. Also briefly described are subsequent published proposals for a reformulation of the quality factor to relate more directly to the *acute* γ-ray exposures from the atomic bombs and for further refinement of the parameter values (and their uncertainties) that determine the shape of the quality factor function. Other recent developments are also mentioned.

1. Introduction

Crew members in space are exposed to a unique and complex radiation environment. In order to estimate the risks to the health of the crew, and to comply with safety standards for acceptable career risks, detailed consideration needs to be given to the types of charged particles encountered in space and the nature of the tracks of ionizations that they produce as they pass through tissue. These track structures are greatly different from those commonly encountered on earth. Risk models require quality factors to account for these differences by relating them to the relatively well-established risk coefficients for human exposures to photons on earth. The quality factor developed by NASA, for use in its cancer risk projection model, incorporates a formula that relates to densely- and sparsely-ionizing components of the radiation tracks. The parameters of the formula have been selected with guidance from experimental data from animal tumors, where possible, and from chromosome aberrations and other effects on cells irradiated in culture. Ongoing research leads to suggestions for future refinement of these parameters as more experimental data become available and also leads to possible modifications to the formula to reduce uncertainties. At present, uncertainty in the values of quality factor is the largest component of uncertainty in assessing the cancer risks from space radiation and this constrains the career limit for the time that NASA crew can spend in space (Cucinotta *et al*. 2013, 2015).

The space radiation environment background has three major components of relevance to exposure of space crew: galactic cosmic radiation (GCR), solar particle events (SPEs), and trapped radiation belts (Schimmerling 2011; NCRP 2014). GCR, which is the component of major concern in deep space beyond the protection of the earth's magnetic field, are mostly highly energetic and composed of all naturally occurring elements; there is a high proportion of protons and helium ions, but elements as heavy as iron are also of concern. SPE consist mostly of protons of moderate energies and occur sporadically with frequencies dependent on the solar cycle and with intensities that vary widely and are not predictable; they are moderately shielded by the material of spacecraft but can be of particular concern during extravehicular activities. Trapped radiation consists of lower energy protons and electrons, which in low earth orbit are mostly shielded by the material of spacecraft. In addition, space crew are exposed to the secondary radiation that is produced when the primary SPE and GCR interact with the spacecraft materials and within the human body.

It is well established that ionizing radiations can cause cancer and other deleterious health effects and that, in general, radiations of high linear-energy transfer (LET)[1] are more biologically damaging per unit absorbed dose[2] than are low-LET radiations. The complex radiation exposure of crew members in space has a substantial high-LET component due to the heavy charged particles in GCR, SPE and the secondary particles which they produce by interactions with the spacecraft and the body. Space permissible exposure limit (SPEL) standards have been set by NASA in order to protect crew members from unacceptable risks from their space exposures (NASA 2015). With respect to cancer, the SPELs require that planned career exposure for radiation shall not exceed 3% risk of radiation exposure induced death (REID), adjusted for age and sex. The risk limit must be met at a 95% confidence level. In order to evaluate the best estimate of REID and its uncertainty distribution, NASA has developed a cancer risk projection model for exposure-induced fatal cancer (Cucinotta *et al*. 2013) and it is on this basis that the career limit of days in space for individual crew members is determined from their exposure histories. The NASA cancer risk projection model is specifically designed to take into account the unique nature of space radiation, which produces particle tracks of great complexity and diversity.

2. Radiation tracks in space and on earth

The solar particles and GCR encountered in space, and their secondary radiations, result in track structures of great diversity as the charged particles pass through the tissue of space crew. These tracks differ greatly from the tracks produces by common radiations on earth. Figure 1 illustrates short segments of tracks from a selection of such space radiation particles. For these examples, the tracks have been generated by the Monte-Carlo track structure simulation code RITRACKS (Plante and Cucinotta 2008; Toburen 2014); they show the high density of ionizations and excitations along the path of the primary charged particle as it interacts with molecules along its path and, also, high density very close to the path due to the overlapping tracks of the lowest-energy delta-ray electrons. At greater distances from the path of the heavy particle average ionization densities decrease progressively due to the stochastic array of higher-energy delta-ray electrons also set in motion by the primary particle. These delta-rays can sometimes extend out to very large distances, depending on the

[1] The linear energy transfer (LET) for charged particles of a given type and energy in a given material, is the quotient of the mean energy lost by the charged particles due to electronic interactions in traversing a unit track length. The unit often used for LET is keV μm^{-1}.

[2] The fundamental dose quantity is absorbed dose, D, defined as the quotient of $d\varepsilon$ by dm, where $d\varepsilon$ is the mean energy imparted by ionizing radiation to matter of mass dm. The SI unit is J kg^{-1} and is given the special name gray (Gy).

velocity of the primary particle, even out to more than about a centimeter for particles of specific energy greater than 1000 MeV/u. The LET of heavy charged particles is given by the Bethe-Bloch stopping power formula[3] (Alloni *et al.* 2014), which shows that the LET increases approximately as the square of the ion charge, Z, and the inverse square of its velocity, V. On the other hand, the maximum range of the delta-ray electrons depends on the velocity of the particle but not its charge. Hence specification of the LET of a particle is seriously inadequate as a description of its track structure; two particles of identical LET but very different charge and velocity will have very different track structures.

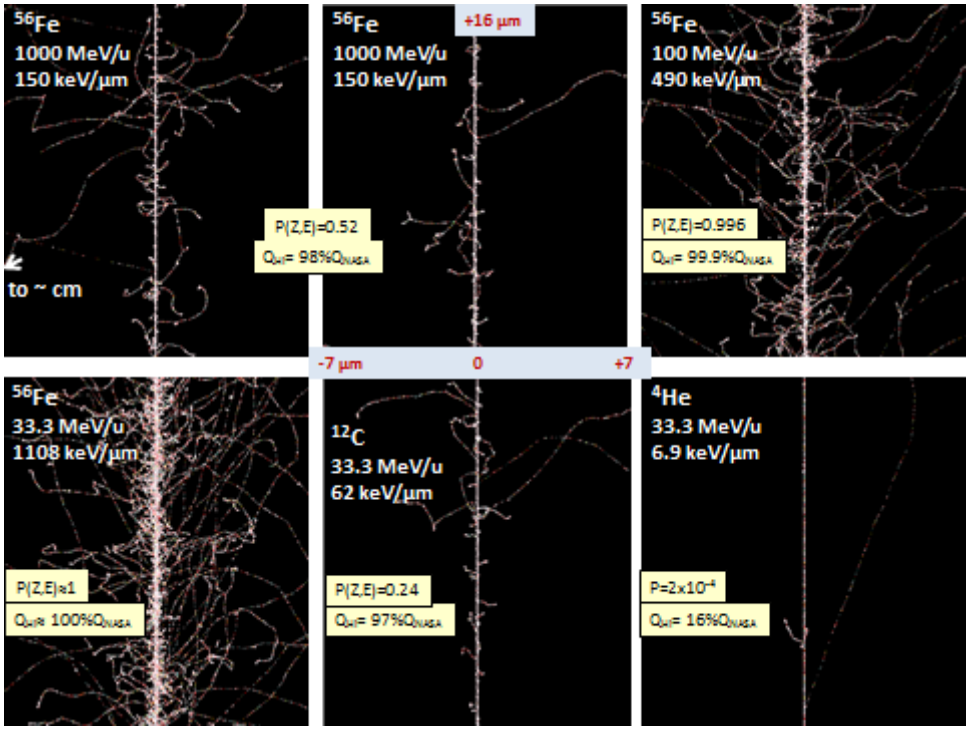

Figure 1: Examples of central portions of track segments from a selection of heavy particles in liquid water. In each case, the specific energy and the LET of the particle is marked. Each track segment shown is about 16 µm in length and the sides of the track are cut off at about 7 µm from the track center; many of the delta-ray electrons travel to much greater distances. The two upper left panels are for identical particles and thereby illustrate the stochastic variation in individual structures. The values marked P(Z,E) represent the average proportion of energy deposited by the particle track that acts in a high-ionization-density manner (evaluated from equations (3) and (4) below). The values marked Q_{hi} represent the percentage of QF_{NASA} that is due to the high-ionization-density component, Q_{Hi}, in equation (5) below for solid cancer risk. See Section 4 below for further explanations. Tracks were generated by the RITRACK Monte Carlo code (Plante and Cucinotta 2008).

[3] The Bethe-Bloch stopping power formula can be written as
$dE/d\ell = 2\pi N_A r_e^2 m_e c^2 \rho(z/A)(Z^2/\beta^2)[\ln(2m_e\gamma^2 v^2 W_M/I^2) - 2\beta^2 - 2S/z - \delta]$,
where Z = charge of the incident particle in units of electron charge; $\beta = v/c$, v being the velocity of the particle and c is the velocity of light; W_M = maximum energy transfer in a single collision; r_e = classical electron radius; N_A = Avogadro's number; I = mean excitation potential; m_e = electron rest mass; z, A, ρ = atomic number, atomic weight and density of material, respectively; $\gamma = 1/(1-\beta^2)^{2/3}$; S = shell factor correction; and δ = density effect correction.

The above HZE radiation tracks encountered in space are greatly different from those experienced on earth. In dramatic contrast, an X- or γ-ray photon such as encountered on earth produces only a single primary electron when it interacts in tissue by Compton scattering or the photo-electric interaction or, at most, a pair of electrons by pair production. Therefore the track structures from photon exposures are simply those of individual electrons, including the lower-energy secondary electrons that are set in motion as the electrons interact and slow down (illustrated in Figures 2a and b). Overall X- and γ-rays are sparsely ionizing and are classified as low-LET radiation. On the other hand, the most densely-ionizing radiation normally encountered on earth is alpha-particles from radionuclide decays. Due to their low energy, however, such alpha particles travel only very short distances (< 0.1 mm in tissue), and so are a health hazard only when the radionuclides are internalized in the body; their delta-ray electrons extend out only to a fraction of a micrometer. Therefore, although these alpha particles are high-LET radiation (~ 60 – 230 keV/μm), their track structures are vastly different from HZE of similarly high LET. LET alone is an inadequate description of radiation quality because it provides only an average one-dimensional description of the ionization density; it ignores the radial distribution of ionizations due to the delta-ray electrons and also the stochastic variability (Curtis 2016).

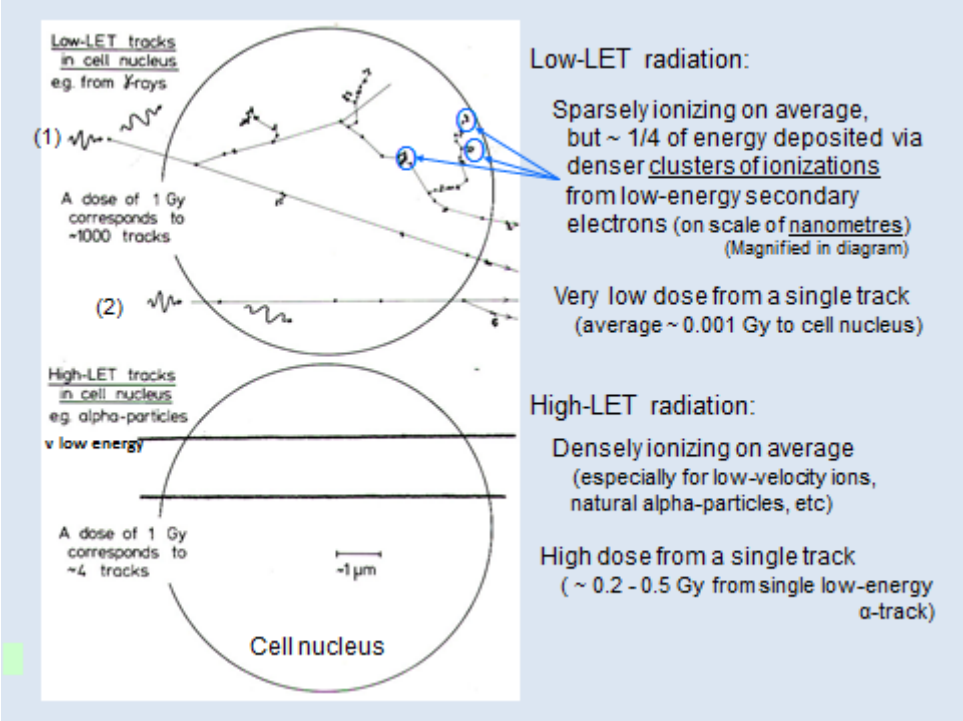

Figure 2a. Schematic diagram of two tracks of electrons from γ-ray interactions (upper portion) or of two low-energy alpha particles from radionuclide decay (lower part) passing through a cell nucleus of diameter 8 μm. (Adapted from Goodhead 1994.)

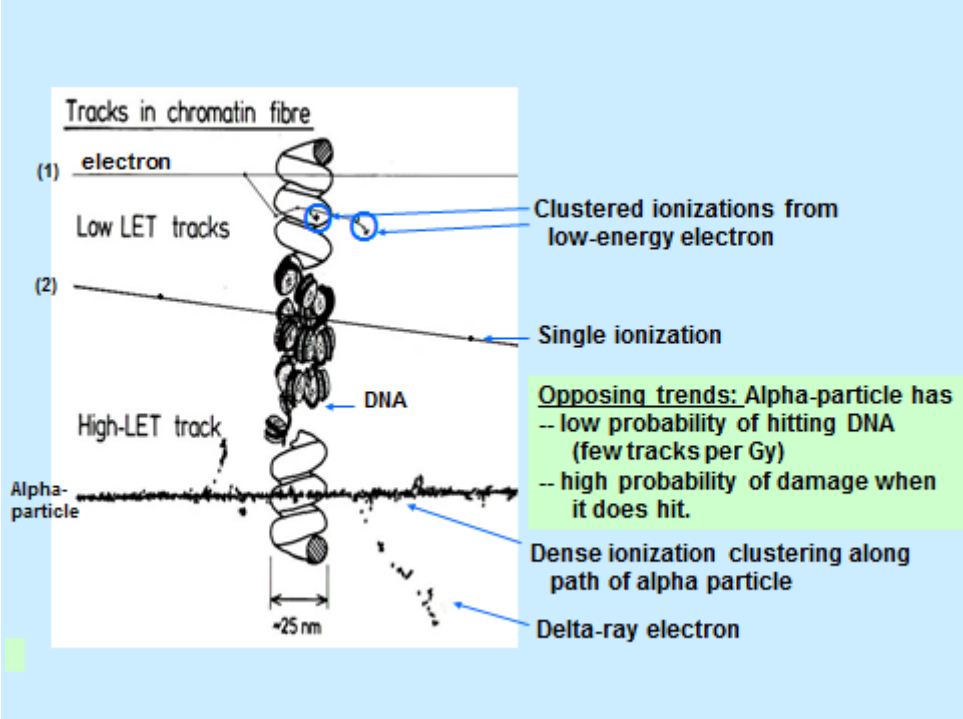

Figure 2b. Schematic diagram at higher magnification of two tracks of electrons (upper portion) or of one low-energy alpha particles (lower part) passing through DNA and chromatin. (Adapted from Goodhead 1988.)

3. Health risks, RBE and quality factor

There is a general paucity of human epidemiological data on the health risks of exposures to high-LET heavy charged particles, due mainly to the small numbers of people who have been exposed to significant quantities of such radiations, with the notable exception of low-energy short-ranged alpha-particles in the lung from inhalation of environmental radon and its short-lived decay products. Other less-common high-LET exposures, such as from other internal alpha-emitters or external neutrons in some occupational situations, from carbon ions as a recent modality of radiotherapy or to astronauts from cosmic-rays, have to date been insufficient in number and uniformity to provide a meaningful database for estimation of cancer risks. There are no statistically significant epidemiology data for late effects from GCR other than for eye cataracts (Chylack *et al*. 2009). In contrast, there is a rich database of epidemiological studies of people exposed to external low-LET γ-rays and X-rays, particularly the survivors of the atomic bombs in Japan as well as from a wide variety of medical and occupational exposure situations. Figure 3 provides a schematic representation of the type of dose response that might be expected for tumor induction after brief low-LET exposure and the corresponding expectations after high-LET exposure. As a consequence, with few exceptions, the usual approach to estimating risk from high-LET radiations has been to scale the estimated low-LET risk coefficient per unit absorbed dose (gray) by a dimensionless factor (>1) representing the enhancement of effectiveness of the high-LET radiation as estimated from available evidence on the relative biological effectiveness[4] (RBE) of the radiations from laboratory and theoretical studies.

[4] The relative biological effectiveness (RBE) of a specified radiation is the ratio of a dose of a low-LET reference radiation to a dose of the radiation considered that gives an identical biological effect. RBE values vary with

When the scaling is from low-LET epidemiological data of cancer risks after brief exposures at moderate to high doses, it is usual to introduce first a reduction factor (often known as the dose and dose-rate effectiveness factor, DDREF[5]) on the assumption that the low-LET risk coefficient is reduced at low doses and/or low dose rates and that the required high-LET risk is either at low doses or independent of dose and dose-rate over the range of interest.

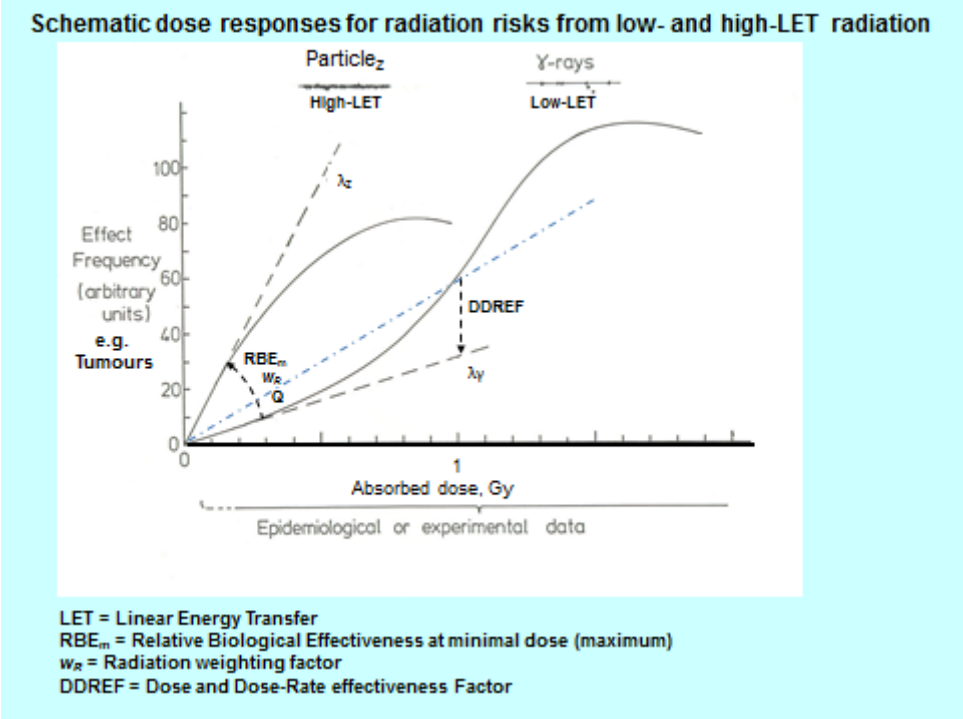

Figure 3. Schematic representation of typical dose responses from low- and high-LET radiations, illustrating the slopes at low doses and the quantities RBE_m, w_R, and Q that are commonly used to scale from the low-LET slope to the high-LET slope. (Adapted from Goodhead 2009.)

On such a basis, the rate of cancer mortality in a given tissue (T) after exposure to a given radiation can be written in a general form as

$$\lambda_Z (D_T, a_E, a) = [\, \lambda_\gamma (a_E, a) / \mathrm{DDREF} \,] \,.\, D_T \,.\, RBE_m \qquad (1)$$

where λ_γ is the rate coefficient (y^{-1} Gy^{-1}) for a linear fit to the acute γ-ray exposure data from epidemiological studies, D_T is the absorbed dose (Gy) to tissue T, α_E is age at exposure, α is attained age, RBE_m is the relative biological effectiveness of the given radiation at minimal dose relative to γ-rays as reference radiation, and DDREF is the dose and dose-rate effectiveness factor.

In view of the paucity of epidemiological data for high-LET radiations, measurements of RBE in experimental systems have been used historically to guide the choice of values of RBE_m to be

---

the dose, dose rate, and biological endpoint considered. In radiological protection, the RBE for stochastic effects at minimal dose (RBE_m) is of particular interest.

[5] The dose and dose-rate effectiveness factor (DDREF) is a judged factor that generalises the usually lower biological effectiveness (per unit of dose) of radiation exposures at low doses and low dose rates as compared with exposures at high doses and high dose rates.

used for estimating risk of stochastic effects. Figure 4 illustrates some common features of curve shape of the experimental dependence of RBE on the LET of the radiation, although it should be emphasized that there is considerable dependence of detail also on other factors such as the biological effect under study (e.g. induction of particular chromosome aberrations, or of particular mutations, or types of tumor), the biological system in use, the level of effect or the dose (since low-LET dose-responses are usually non-linear and high-LET response tend more towards linearity), the dose rate and the velocity of the charged particles of a given LET. The latter variation in RBE at a given LET is the consequence of the differences in track structures between particles that have the same LET but different charge and velocity.

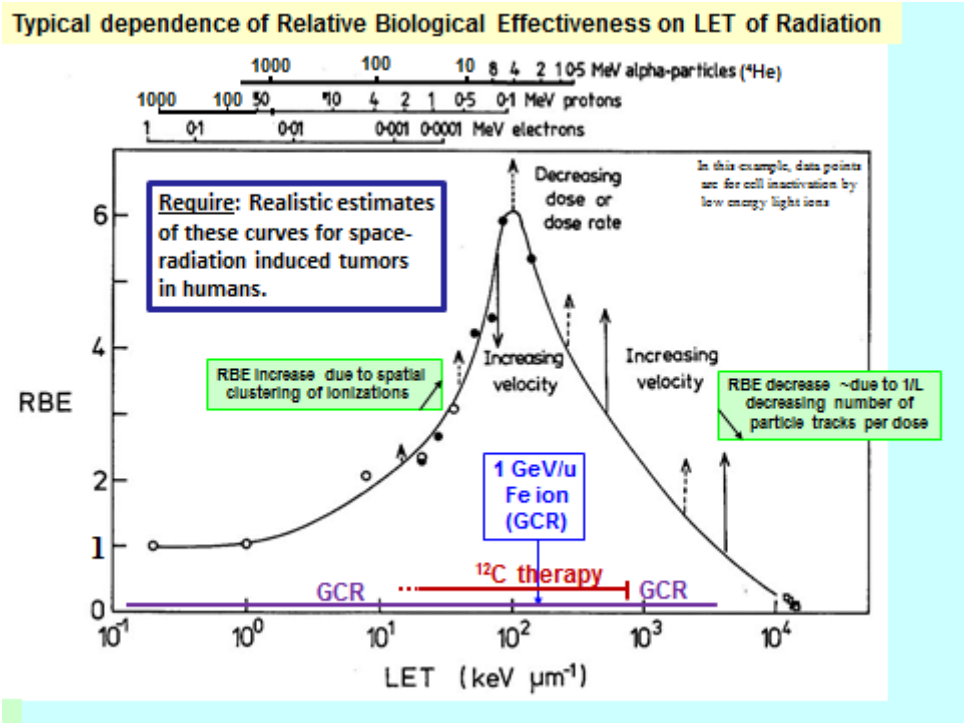

Figure 4. Illustration of features commonly observed for the variation of relative biological effectiveness (RBE) with LET. (Adapted from Goodhead 1994.)

For the purpose of prospective radiation protection, the International Commission on Radiological Protection (ICRP) has defined the dimensionless quantity radiation weighting factor, w_R, in order to convert absorbed dose (in Gy) to equivalent dose (Sv) in a tissue and to effective dose (Sv) in the body (ICRP 2007). The ICRP-specified values of w_R are 1 for all photon and electron radiations, 2 for protons and charged pions and 20 for all alpha-particles, fission fragments and heavy charged particles (ICRP 2007). This simplified set of values was based on judgement from the available data on RBE, but with recognition of the simplicity and limited accuracy required for systematic application for radiation protection planning. For operational radiation protection (measurements and assessment of doses in the body), a quality factor, Q, was defined as a continuous function of the LET of the radiation in order to give broadly similar results for measured radiation fields (ICRP 2007). It is recognised that different particles of the same LET may show differences in RBE, but this is neglected in specifying Q as a simple function of LET because of the simplicity and limited accuracy required for radiation protection on earth and the small range of high of high-LET exposures encountered on earth. The ICRP values of w_R and Q are summarized in Figure 5.

Additionally, the ICRP states that for the purposes of *risk estimation* under specific circumstances the best estimate of RBE for those circumstances should be used based on all available knowledge.

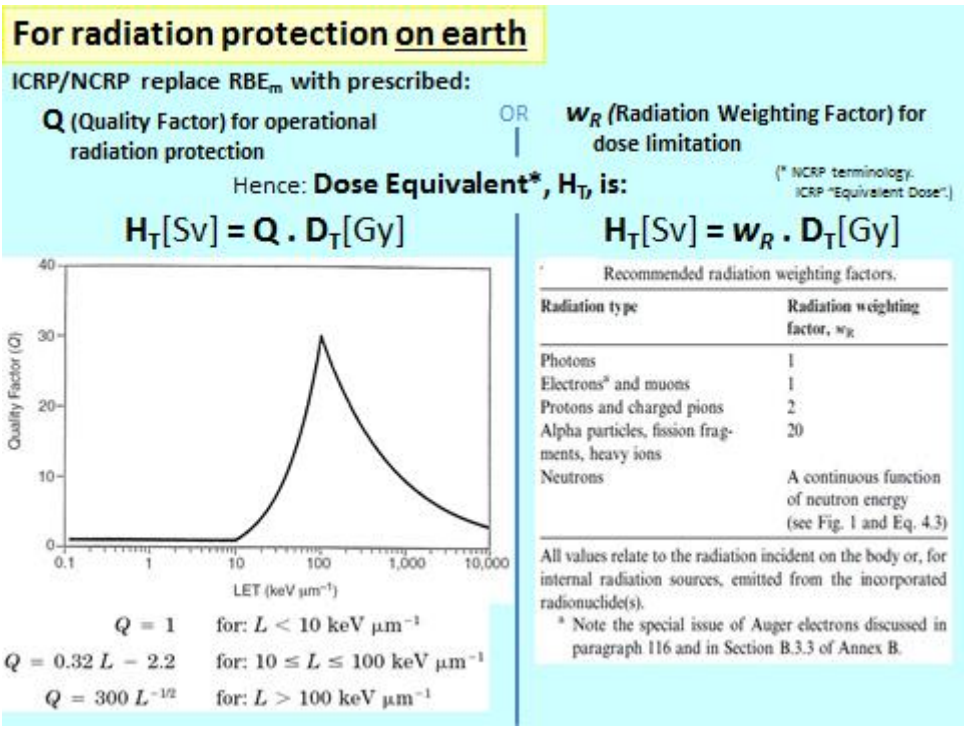

Figure 5. Values of radiation weighting factor, w_R, and quality factor, Q, in the system of radiation protection used on earth, as recommended by the ICRP (2007).

It is known that particles of different charge but the same LET can induce different levels of response for some cancer-surrogate measureable endpoints. Differences can be particularly large for the heavy charged particles encountered in space, due to the large differences in track structure that can exist between particles of the same LET but different charge and velocity. Incorporation of these track structure features is a key conceptual difference between the quality factor used by NASA (QF_{NASA}) for projection of risk from space exposures and the quality factor recommended by the ICRP (Q(LET)) for operational radiation protection on earth.

4. NASA quality factor, QF_{NASA}

Because of the unusual and diverse nature of the radiations encountered in space, especially the large high-LET component, a more precise analytic form of quality factor, QF_{NASA}, has been developed for space radiation and applied in the NASA risk projection model for radiation exposure induced death from cancer (REID) (Cucinotta *et al*. 2013; Cucinotta 2015a). In the NASA Cancer Risk Projection Model, NSCR-2012 (Cucinotta *et al*. 2013), when absorbed dose D_T is deposited in tissue T, by a particle of charge Z and energy/nucleon E, equation (1) becomes

$$\lambda_Z (D_T, a_E, a) = [\, \lambda_\gamma (a_E, a) / \mathrm{DDREF} \,] \,.\, D_T \,.\, QF_{NASA} \qquad (2).$$

In order to obtain REID and its uncertainty distribution for a specific scenario of space radiation exposure, equation (2) is summed over the particle fluence spectrum (as track segments) responsible for the dose to tissue T and over all tissues and the time of the exposure.

The NASA quality factor for particles of charge Z and energy/nucleon E is specified as

$$QF_{NASA} = [\ 1 - P(Z,E)\ ]\ +\ [6.24\ (\ \Sigma_0/\alpha_\gamma\ )\ /\ LET\ ]\ .\ P(Z,E) \qquad (3)$$

$$\text{where} \quad P(Z,E) = (1 - \exp(-Z^{*2}/\kappa\beta^2))^m .\ (1 - e^{-(E/0.2)}). \qquad (4)$$

β is the velocity of the particle relative to the speed of light and Z* is the effective charge[6]. The 'height' parameter Σ_0/α_γ and the so-called 'shape' parameters κ and *m* will be discussed below in Section 4.2. The main[7] functional form of P originates from the amorphous track structure model of Katz *et al*. (1971). The NASA quality factor was reviewed by the National Academies (NA/NRC 2012) and approved by the NASA Chief Health and Medical Officer for uses at NASA (Cucinotta 2015a).

Equation (3) separates the quality factor into two components,

$$QF_{NASA} = Q_{Low} + Q_{Hi} \qquad (5)$$

These implicitly represent the low-ionization-density and high-ionizing-density components of the particle track, respectively (Cucinotta *et al*. 2017). Parameter P(Z,E) can be interpreted as the proportion of the particle track that acts in a high-density like manner and, conversely, (1 – P) as the proportion that acts in a low-density like manner. The above formulation of QF_{NASA} and its use in the risk-projection equation (2) implicitly assumes that the low-density component of the tracks act with the same effectiveness per unit absorbed dose as do the reference γ-rays. By contrast, the high-density component acts with weighting increased by the factor of $6.24(\Sigma_0/\alpha_\gamma)/LET$. The following two sections will discuss each of these two components in turn.

4.1 Low-ionization-density component of QF_{NASA}

The low-ionization-density component in equations (3) and (5) is due to the non-overlapping delta-ray electrons that can be considered to act separately from the main path of the heavy charged particle. In the NASA cancer risk projection model equation (2), this component is assigned the same biological effectiveness per unit absorbed dose as the reference γ-rays for which human cancer risk coefficients have been derived from epidemiological studies of the atomic-bomb survivors. How reasonable is this assumption in the light of comparisons between the energy spectra of the delta-ray electrons from HZE, on the one hand, and the primary electrons produced by the γ-ray interactions, on the other? The number spectrum of delta-rays of initial energy E_e, produced by a heavy charged particle, falls off approximately as $1/E_e^2$, up to the maximum delta-ray energy permitted by the kinematics of the interaction. Is it reasonable to expect this wide and heavily skewed spectrum of electron energies to act with the same biological effectiveness as the first-collision electron spectrum produced by interactions of the reference γ-rays?

The value of radiation weighting factor, w_R, and quality factor, Q, recommended by ICRP for use in radiation protection is unity for all photon and electron radiations, irrespective of energy. It is, however, well recognized that the relative biological effectiveness of photons and electrons does depend on their energy in a variety of experimental systems and is likely to do so also for human

[6] The effective charge takes into account the reduced charge of a particle at very low specific energies (<~ 0.2 MeV/u) due to charge exchange, using the Barkas correction.

[7] A parametric 'thindown' term, $(1 - e^{-(E/0.2)})$, is added in equation (4) to reflect reduced biological effectiveness near the end of the residual range of stopping ions due to the narrowness of their tracks in this region (Cucinotta *et al*. 2013).

cancer induction. It is acknowledged that the more precise values should be used for risk estimation, when possible. The NCRP has recently considered the experimental, theoretical and epidemiological evidence for variation of RBE with photon or electron energy and from this information provided guidance on probability distribution functions for the effectiveness ratio for risk of human cancer (NCRP 2018) by photons in a variety of lower-energy bands, relative to ^{60}Co γ-rays. RBEs measured in many experimental systems are seen to increase more than two-fold as the photon energy decreases to very low energies. This increase is presumably due to the increase, with decreasing photon energy, of the proportion of low-energy first collision electrons and the consequent increase in the proportion of absorbed dose deposited by very low-energy electrons (with energies of a few hundred to a few thousand electron-volts) in the electron slowing-down spectrum. Such very low-energy electrons have very short ionisation mean free paths (a few nanometers) and are particularly efficient at producing clustering of ionisations on the scale of the DNA helix and hence DNA double-strand breaks, both simple and complex (Goodhead 1994, 2009).

As explained above, the number spectrum of delta-ray electrons from heavy charged particles is very heavily skewed to low energies ($\sim 1/E_e^2$) and the energy-weighted (or dose-weighted) spectrum is also skewed ($\sim 1/E_e$). On this basis alone one might expect this spectrum of electrons to be biologically more effective than the first collision electron spectrum from ^{60}Co or atomic bomb γ-rays. However, in making such an inference, it should be borne in mind that the lowest-energy delta-ray tracks are entirely very close to the path of the heavy particle itself and, at least for higher-charge particles, are likely also to be very close to or overlapping with other delta rays. Such delta-rays are likely to be partitioned by equations (3) and (4) to the high-ionisation-density component of the heavy particle track (as Q_{Hi} in QF_{NASA}) and thereby excluded from the present consideration of the low-ionisation-density component. From rough comparison of the energy spectrum of the higher-energy, non-overlapping, delta-ray electrons produced by heavy charged particles with the energy spectrum of first collision electrons from ^{60}Co or atomic bomb γ-rays (as presented by NCRP 2018), it appears reasonable to suggest that the delta rays constituting the first term in equations (3) and (4) will mostly have similar biological effectiveness to that of the γ-rays. Particles of low charge, especially protons, and intermediate energies (< ~ 100 MeV/u) may deviate slightly from this general expectation because their very low-energy delta rays are unlikely to overlap.

4.2 High-ionization-density component of QF_{NASA}

We now consider the second term in equations (3) and (5), Q_{Hi}, representing the densely-ionizing component of the heavy charged particle track. It is dependent on the charge (Z), velocity (β) and LET of the particle and also on the values assigned to the parameters Σ_0/α_γ, κ and *m*. The role of these three fitted parameters is illustrated qualitatively in Figure 6 with respect to a notional relationship of quality factor versus Z^{*2}/β^2. For simplicity of the illustration the same curve has been used here as previously in Figure 4 for RBE versus LET[8]. In practice, the same parameterized form as QF_{NASA} (equation (3)) was used to fit available experimental RBE data for charged particles of varying velocity and charge in order to guide the choice of values of the Σ_0/α_γ, κ and *m* parameters for specification of QF_{NASA} in the risk model (Cucinotta *et al*. 2013).

[8] LET and Z^{*2}/β^2 are closely related because, in the Bethe-Block stopping power formula, LET is approximately proportional to Z^2/β^2, with deviations confined essentially to very low-velocity particles or to relativistic corrections. Plotting quality factor, or RBE, against Z^{*2}/β^2 eliminates much of the multiplicity that arises between particles of the same LET but different charge and velocity, as discussed by Curtis (2016) and in Section 5.3 of Cucinotta et al. (2013).

As illustrated in Figure 6, the single compound parameter, Σ_0/α_γ, controls the peak height of the quality factor curve, as illustrated in Figure 6, and is set for the estimated maximum value of QF_{NASA} of the most-effective particle for induction of fatal cancer. In practice, it is selected from fits to available experimental data-sets as a single parameter (Σ_0/α_γ), which represents the maximum effect cross-section of the most-effective particle normalized to the effectiveness of low dose-rate γ-ray exposures[9].

Regarding the two dimensionless "shape" parameters, *m* governs the steepness with which the quality factor (or RBE) curve increases with increasing Z^{*2}/β^2, and κ determines the position of the peak value along the Z^{*2}/β^2, axis. For QF_{NASA}, these too were selected from fits to available experimental data-sets.

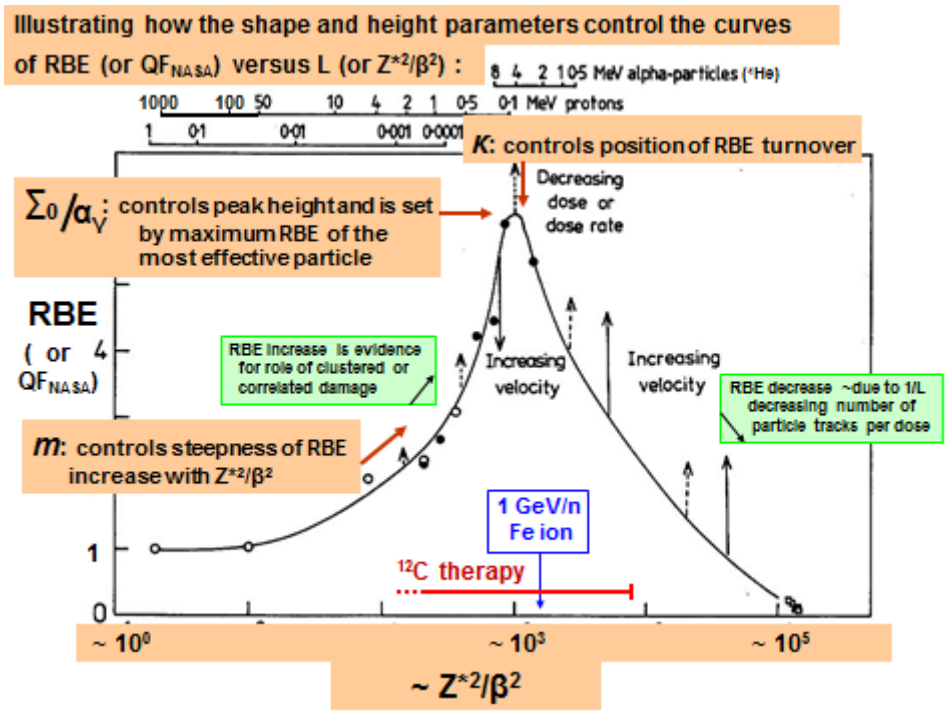

Figure 6. Schematic illustration of the role of the parameters Σ_0/α_γ, κ and *m* in determining the shape of the RBE (or QF_{NASA}) versus Z^{*2}/β^2 curve.

Table 1 shows the values selected for the above three parameters for QF_{NASA} in the current NASA risk projection model for risk of exposure induced death from cancer, NSCR-2012 (Cucinotta *et al*. 2013). Different values were selected for leukemia as compared to solid cancers because the experimental data from animal tumor studies (as well as some human evidence) show that the RBEs of high-LET radiations for leukemia induction are much lower than for solid cancers in general. Additionally, distinct values of κ were selected for low-charge particles ($Z \leq 4$). The parameter values in Table 1 (and their uncertainty distributions) were set as subjective estimates from the results of radiobiology experiments available at the time of establishing the risk model. The values of *m* were estimated from *in vitro* mammalian cell experimental data on chromosome aberrations, hprt mutations and neoplastic transformation, the values of *κ* from data on *in vitro* mammalian cell chromosome aberrations, hprt mutations and neoplastic transformation and *in vivo* mouse Harderian

[9] The numerical factor 6.24/LET enters into equation (3) in association with the parameter Σ_0/α_γ due to comparison of effect cross-section (per unit fluence) for heavy particles (Σ_0, in μm^{-2}) with effect coefficient (per unit absorbed dose) for γ-rays (α_γ, in Gy^{-1}).

gland tumors, and values of Σ_0/α_γ from data on *in vivo* mouse tumors and *in vitro* mammalian cell chromosome aberrations and gene mutations (Cucinotta *et al*. 2013).

Table 1. **Parameter values for QF_{NASA}.**

Parameter	Solid Cancer	Leukemia
m	3	3
κ	550 (1000)*	550 (1000)*
Σ_0/α_γ, $\mu m^2 Gy$	7000/6.24	1750/6.24

* Values in parenthesis are distinct values for particles of charge ≤ 4.

4.3 Evaluations of QF_{NASA}

The variation of QF_{NASA} with LET is shown in Figure 7 for a selection of heavy charged particles, namely hydrogen, carbon, silicon and iron, in each case separately for solid cancers and leukemia. Also shown, for comparison is the corresponding ICRP quality factor, which depends only on LET and is independent of the particle charge (ICRP 2007). It is readily apparent from comparisons across panels that there are large differences in QF_{NASA} between particles of the same LET but different charge, and also large differences compared to the ICRP quality factor. These features of QF_{NASA} are a result of its approach to take into account the large differences in track structure, including between different particles of the same LET, and to set its parameters on the basis of available data on the relative effectiveness of HZE in a variety of experimental systems.

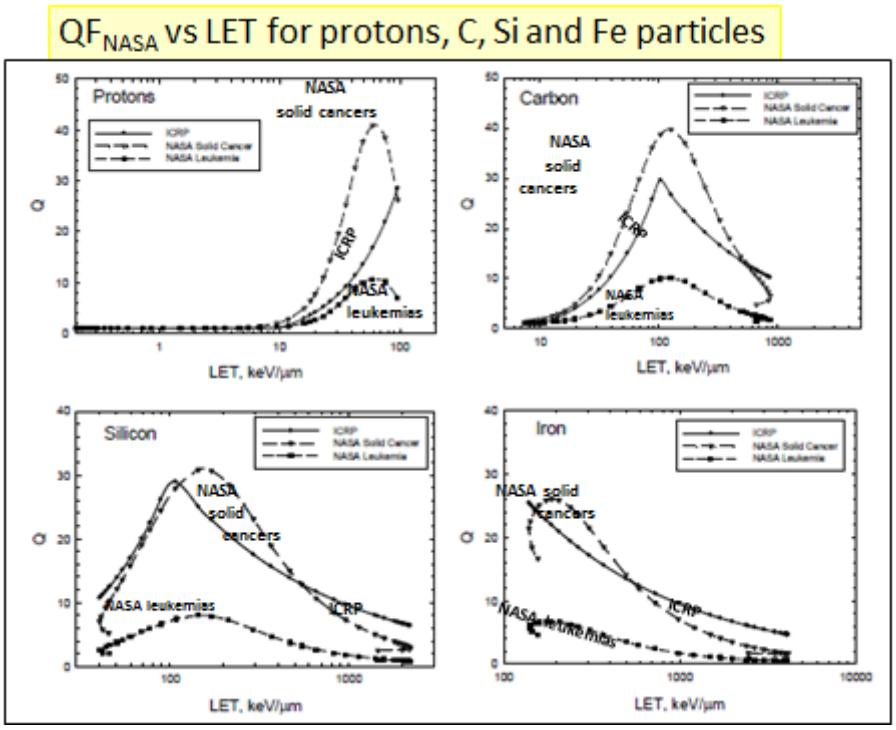

Figure 7. Comparison of LET dependence of QF_{NASA} for four different charged particles (protons, carbon, silicon and iron) for solid cancers and for leukemias, as evaluated by the NSCR-2012 risk model (Cucinotta *et al*. 2013). Also shown for comparison is the Q versus LET relationship recommended by the ICRP for operational radiation protection on earth (ICRP 2007); this is independent of particle type and therefore identical in each panel. (Reproduced, with permission, from Cucinotta *et al*. 2013.)

Examples of the proportion of the energy deposited by particle tracks that acts in a high-ionization-density manner, P(Z,E), are marked in Figure 1 for the sample of charged particles illustrated there (evaluated from equation (4)). Also marked are the percentage contributions made by Q_{Hi} to the value of QF_{NASA} for those particles for solid cancer risk (from equations (3) and (5)). It is notable how totally dominant the high-ionization-density component can be, even when a substantial proportion of the particles' energy deposition is via low-ionization-density delta rays, such as in the case of 1000 MeV/u Fe particles. At the other end of the extremes are, say, 1000 MeV protons, which produce essentially no high-ionization-density component at all ($P(Z,E) = 2 \times 10^{-9}$, $Q_{Hi} = (6 \times 10^{-3})\%$ QF_{NASA}). Such protons (not shown in Figure 2) produce only isolated delta-ray electrons, with negligible overlap in small volumes, in much the same way as do high-energy photons, except for the long-distance rectilinear correlation along the path of the protons. In general, for all particles, the high-density component is somewhat less dominant for leukemias than it is for solid tumors because of the lower value assigned to Σ_0/α_γ (Table 1).

The NASA space cancer risk model NSCR-2012 is used to calculate the cancer risk of exposure induced death (REID) at the upper 95% confidence limit (interpreted as the 97.5 percentile) for comparison with the space permissible exposure limit (SPEL) standards set by NASA (NASA 2015). For operational purposes, these calculations can be applied to evaluate the remaining mission duration permitted for individual space crew for a specific planned mission scenario, based on the crew member's previous radiation exposure history. Therefore, a crucial aspect of the risk model is the probability distribution function (PDF) of REID for the particular conditions and determination of its 97.5 percentile. This requires assignment of uncertainties to the parameters of the risk model, including those that determine the quality factor, QF_{NASA}. Definition of QF_{NASA} as described above provides a convenient parameterized form for assignment of uncertainties, mostly in the form of PDFs, for the individual parameter values. In the NSCR-2012 risk model, these PDFs were assigned on the basis of subjective judgements from available experimental information (Cucinotta *et al*. 2013). Discussion of these uncertainty distributions is beyond the scope of the present article, but it should be apparent that their choice and efficiency of computation are highly pertinent to determination of the 97.5 percentile of REID. Recent computational research, presented as a poster at the 2017 Annual Meeting of the Radiation Research Society, has led to suggestions that revision of the form of the uncertainty distribution of the κ parameter from normal to log-normal and addition of a correlation constraint on the κ and m parameters leads to improved description and computational convenience of the high-REID tail of the risk distribution (M.R. Shavers, personal communication).

Despite this detailed approach to defining QF_{NASA}, quality factor remains by far the largest contributor to uncertainties in evaluations of REID for travel beyond low earth orbit, as illustrated in Table 2 for a particular mission scenario in deep space. A major goal of current research in carcinogenesis by HZE is to reduce the uncertainties in QF_{NASA}, with the expectation that this will increase the permitted time in space flight for space crew, sometimes described as "safe days in space" (Cucinotta 2015a). In the future, NASA will report the metric "Permissible Mission Duration", which is that duration of a specific mission beginning on a specific launch date for a male or female astronaut of a specific age that results in a projected exposure exactly equal to the NASA SPEL, considering the astronaut's previous occupational exposures (M.A. Shavers, personal communication).

Table 2. Example of contributions of various uncertainties to a probability distribution function for fatal cancer risk, as evaluated by the NASA risk model NSCR-2012 in Cucinotta *et al*. 2013. The point estimate is headed "Expected".

[This example is for 40-y-old females on a 1-y mission at solar minimum in deep space with a 2 g/cm^2 aluminium shield.

Uncertainties considered	Expected	Mean	Median	STD	Lower 95%	Upper 95%	Fold Uncert.
Epidemiology, Transfer	2.60	2.24	2.09	0.82	0.62	4.0	1.53
Epidemiology, Transfer, DDREF	2.60	1.59	1.36	0.76	0.40	3.37	1.30
Q only	2.60	2.85	2.24	2.22	0.92	7.96	3.06
Q and Physics	2.60	2.89	2.26	2.22	0.92	8.10	3.12
All uncertainties	**2.60**	**2.03**	**1.50**	**1.92**	**0.40**	**6.34**	**2.44**

5. Proposals for further development of quality factor for space radiation

Since the formulation of the NASA Cancer Risk Projection Model NSCR-2012 (Cucinotta *et al*. 2013) and its implementation for comparison with the space permissible exposure limit (SPEL) standards set by NASA (NASA 2015), ongoing research has continued to seek additional data and methods for potential further reduction in uncertainties in risk projection. Sections 5.1 and 5.2 summarize recent suggestions that relate to specification and evaluation of quality factor. Section 5.3 summarizes a suggestion that has been made for real-time estimation of an approximate dose-averaged quality factor for the GCR component of exposure during a mission.

5.1 New approach to quality factor: $Q_{\gamma,acute}$

As can be seen from Table 2, another substantial source of uncertainty in the NASA risk projection model for REID is the value of DDREF in equation (2). In the risk model, DDREF is applied to adjust the risk coefficients for low-LET exposures at high dose-rates and moderate to high doses, obtained from epidemiological studies such as of the A-bomb survivors in Japan, to the low dose rate (low fluence rate) exposures in space, before multiplication by the quality factor, QF_{NASA}, for space radiation (as illustrated schematically in Figure 3). The following alternative approach has subsequently been suggested (Cucinotta 2015b; Cucinotta *et al*., 2016).

If it is assumed that the first and second terms on the right-hand side of equation (3) represent the relative effectiveness of the low-ionization-density and the high-ionization-density parts of the heavy particle tracks, respectively, and that the high-density part is not dependent on dose rate, then the risk coefficients for this part of the tracks can be estimated by direct scaling from the coefficients of acute γ-ray exposures at moderate to high doses (about 0.5 – 3 Gy), without any need to invoke a DDREF parameter. DDREF still needs to be employed for the low-ionization-density part of the track.

In this suggested new approach (illustrated in Figure 8), equation (2) is re-written as

$$\lambda_Z (D_T, a_E, a) = \lambda_\gamma (a_E, a) . Q_{\gamma,acute} . D_T \qquad (6)$$

where $Q_{\gamma,acute} = [1 - P(Z,E)]/DDREF + [6.24 (\Sigma_0/\alpha_{\gamma,acute}) / LET] . P(Z,E)$ (7).

As before, $\Sigma_0/\alpha_{\gamma,acute}$ is obtained by fitting to available data as a single parameter[10], but it now sets the maximum effect cross-section of the most-effective particle normalized to the effectiveness of *acute* γ-ray exposures at doses in the range about 0.5 – 5 Gy. Equation (6) is identical to equation (2) within the approximation that ($\Sigma_0/\alpha_{\gamma,acute}$) ≈ (Σ_0/α_γ) /DDREF. When this new formulation was introduced, the shape parameters, κ and *m*, were left unchanged (Cucinotta 2015b; Cucinotta *et al*. 2016).

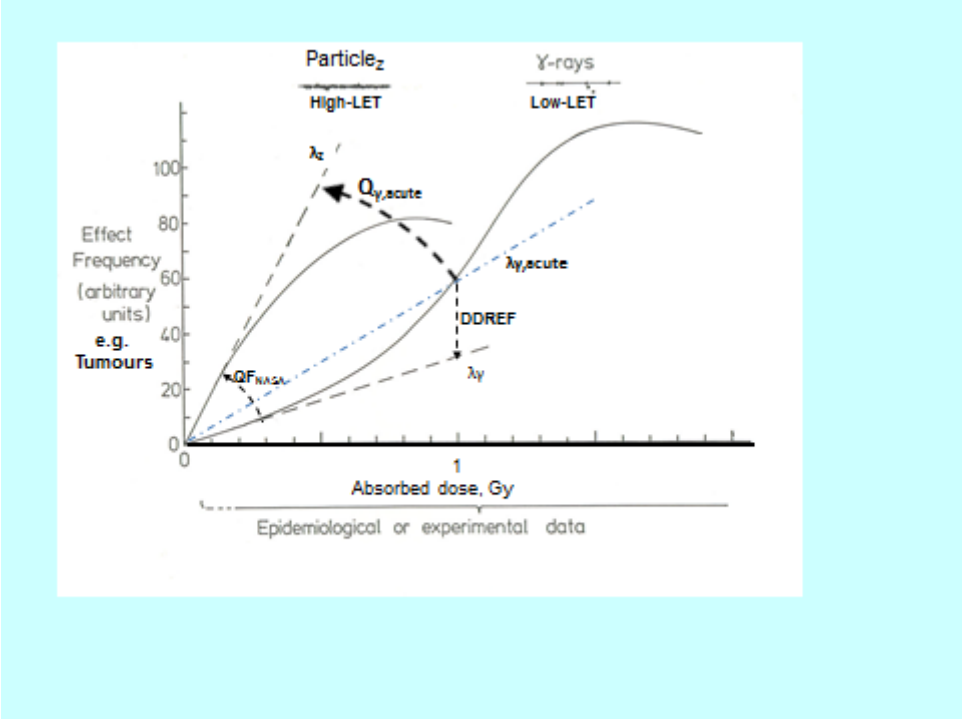

Figure 8. Schematic representation of typical dose responses from low- and high-LET radiations as in Figure 3, but now showing the proposed direct scaling from the acute γ-ray slope at higher doses to the HZE-particle slope, using the quality factor $Q_{\gamma,acute}$, as compared to the scaling in the NSCR-2012 risk model, which uses DDREF and QF_{NASA}.

This new approach to quality factor, as well as some changed methods for uncertainty analysis, has been incorporated as potential modifications or updates to the NSCR-2012 risk projection model and the modified model denoted as NSCR-2014 (Cucinotta 2015b). With the mean value of $\Sigma_0/\alpha_{\gamma,acute}$ set at 2700/6.24, evaluation of the cancer risk model for a 1-year space mission showed that, on their own, the changes to methods of uncertainty analysis increased predictions of %REID by about 35% and of the upper 95% confidence level by about 25% when compared to NSCR-2012, but that introduction of the new approach to quality factor, $Q_{\gamma,acute}$ (equation 6), then greatly reduced these higher predictions by about 40% and 50%, respectively (Cucinotta *et al*. 2015). The net effect was that NSCR-2014 predictions were about 25% and 40% lower, respectively, than the corresponding NSCR-2012 predictions. Figure 9 shows such a comparison of %REID distributions calculated by the two models. It can be seen that both the central value and the uncertainties are reduced with the later model, the reduction being mainly due to the introduction of $Q_{\gamma,acute}$ in place of QF_{NASA}/DDREF.

[10] In the present article this new proposed parameter is given the notation $\Sigma_0/\alpha_{\gamma,acute}$ to distinguish it from the parameter Σ_0/α_γ used for the original model; this distinction of notation is not made in the cited publications (Cucinotta 2015b; Cucinotta *et al*. 2016).

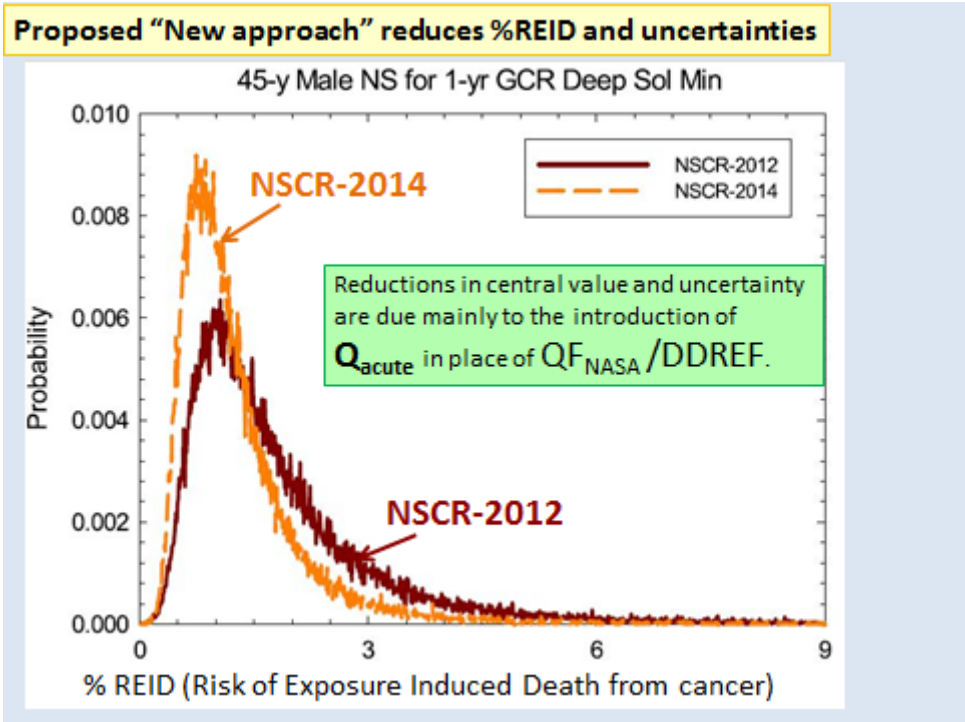

Figure 9. Comparison of probability distribution function for fatal cancer (for a specified one-year mission) as evaluated by the NASA risk model NSCR-2012 and the later proposed model NCSR-2014, in which QF_{NASA}/DDREF is replaced by Q_{acute}. (Modified from Cucinotta *et al*. 2015.)

5.2 Refinement of quality factor model parameter values and uncertainties

As more experimental data on relevant biological effects of HZE become available they can be applied to provide further guidance for estimation of central values and uncertainty distributions of parameters used to define the quality factor relationship.

It is impractical to carry out tumor induction studies in animal models for all but a small selection of the large number of particle types and wide range of energies in the primary and secondary radiations in space. Consequently, *in vitro* surrogate endpoints have been used to investigate details of the radiation quality dependence of RBEs and it is largely on judgements from such data that the values of the shape parameters, κ and *m*, and their uncertainties were estimated for QF_{NASA} for the NSCR-2012 risk projection model (see sections 4.2 and 4.3 above). Subsequently, and using the same parameterized form of radiation quality dependence as in NSCR-2014 (i.e. equation (7)), Cacao *et al*. (2016) made further systematic analyses of the best parameter values of κ and *m* to fit *in vitro* data and predict RBEs of HZE exposures, particularly for induction of chromosome aberrations but also for cell transformation and gene induction. Figure 10 shows how the predicted values of RBE_{acute} (i.e. the RBE relative to acute γ-rays) vary with LET for a variety of heavy charged particles. This diagram illustrates dramatically how substantially the RBE can differ between different particles of the same LET. As stated previously, these differences are due to the large differences in track structure, associated particularly with the lateral spread of the energy by delta-ray electrons.

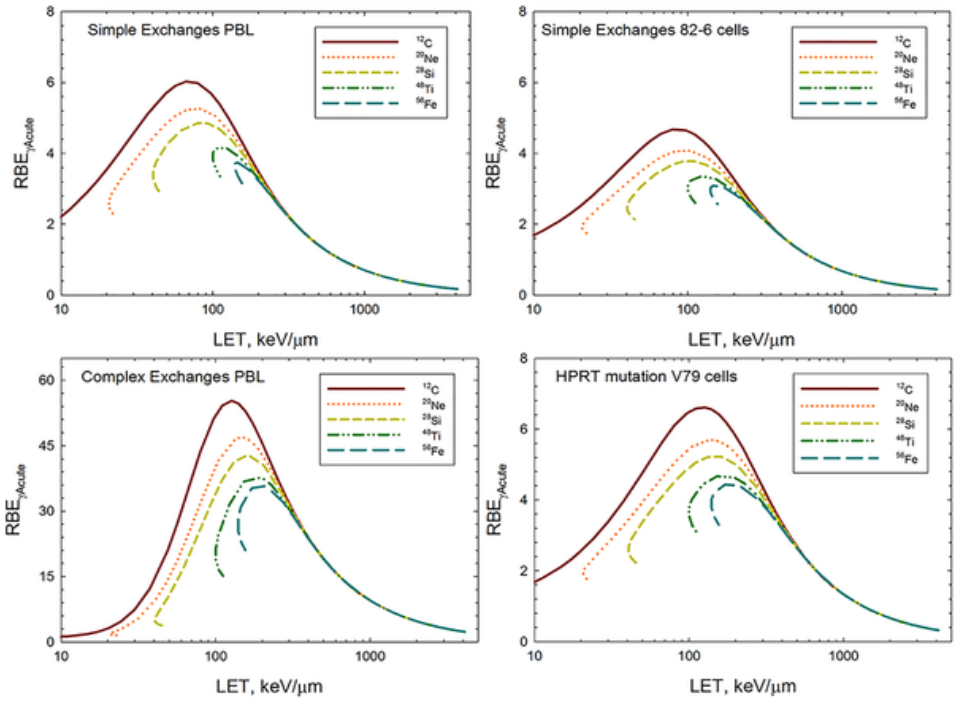

Figure 10. Predicted dependence of RBE_{acute} on LET for a variety of charged particles and several *in vitro* biological endpoints of relevance to cancer induction. (Reproduced, with permission, from Cacao *et al*. (2016).)

By far the most comprehensive set of experiments on tumor induction by HZE of varying charge and energy was completed by Chang *et al*. (2016) for mouse Harderian tumors. Figure 11 shows the set of results, plotted as tumor prevalence versus particle traversals per cell nucleus. Although the Harderian gland does not exist in humans, this data-set is deemed to be particularly valuable because of the wide range of charged particles that were used and the consequent information that they can provide on the shape parameters, κ and *m*. Cucinotta *et al*. (2017) analysed this dataset, to provide further guidance on the values and uncertainties of κ and *m*, together with the above results from Cacao *et al*. (2016) for surrogate endpoints. Estimates were then made of the value of the height parameter, $\Sigma_0/\alpha_{\gamma,acute}$, from a wide range of mouse tumor data in the literature, including data that were used for development of the NSCR-2012 and NSCR-2014 risk models, but now extended by the later data for the Harderian tumors (Chang *et al*. 2016), recent results for colorectal and intestinal tumors (Suman *et al*. 2016) after HZE exposures, and results from last century for several tumor types induced by low-energy proton recoils from fission neutron exposures. The cumulative distribution function (CDF) (Figure 12) of $\Sigma_0/\alpha_{\gamma,acute}$ for all solid cancers gave a mean value of (4,728 ± 1378)/6.24. The mean value for liver cancers (13,296 ± 4739)/6.24 was much larger and more dispersed than for any other tumors and substantially raised the overall mean. When liver cancers and Harderian[11] tumors were excluded from the CDF, the mean for all the remaining solid cancers became (2,897 ± 357)/6.24. The authors recommended that this latter reduced CDF be used for space mission risk predictions, while the more conservative estimate for liver cancer risk be considered in a separate calculation[12] (Cucinotta et al. 2017).

[11] Harderian gland tumors were excluded because humans do not have such a gland.

[12] The rationale for separating out liver cancers was based also on particular issues relating to extrapolation of liver cancer risks from the atomic bomb survivors (with very high background incidence in Japan) to the US population and astronauts, as well as potential large sex dependence in both the human and mouse data.

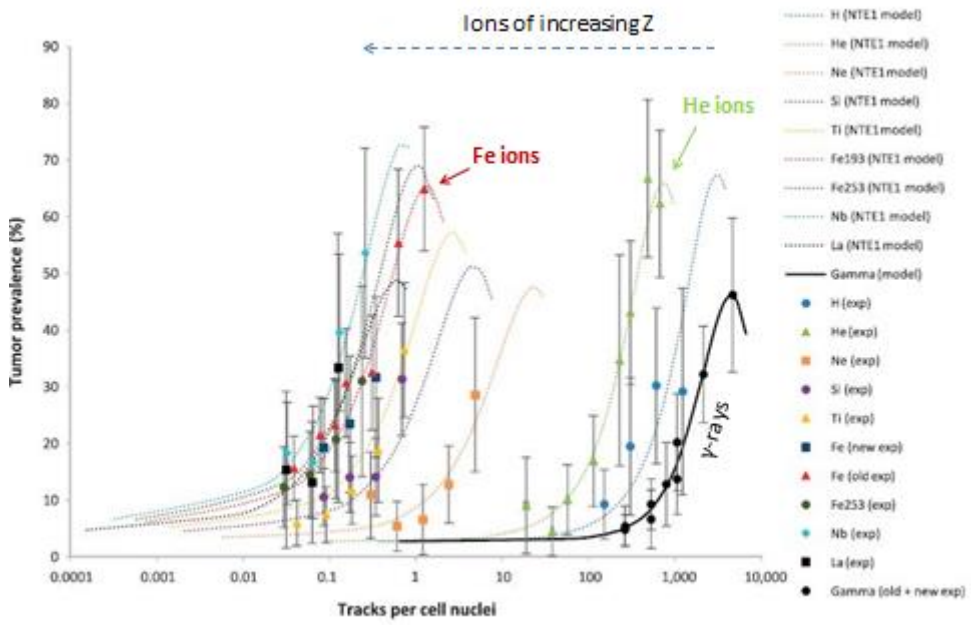

Figure 11. Prevalence of Harderian gland tumors in mice exposed to heavy charged particles as a function of particle fluence (heavy particle tracks per cell nucleus). (Modified from Chang *et al*. 2016).

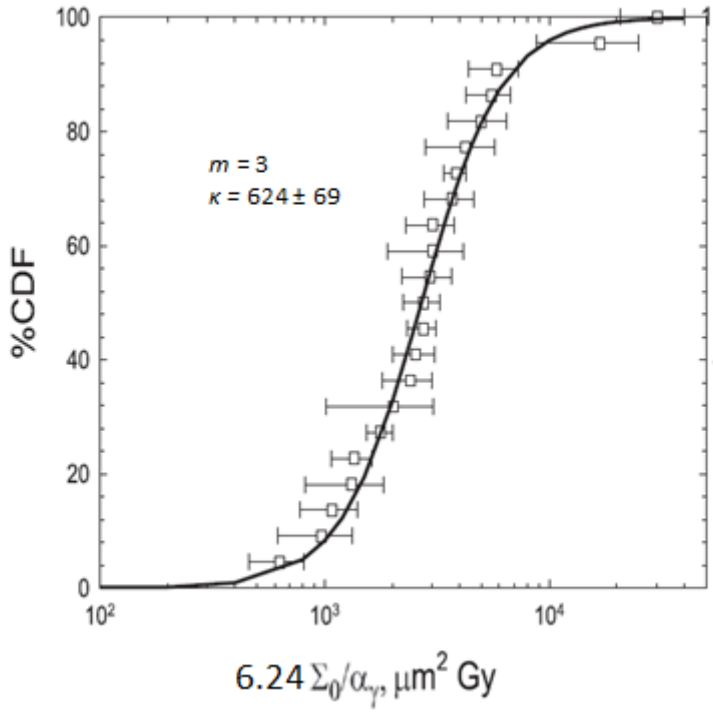

Figure 12. Cumulative distribution function of parameter $6.24\Sigma_0/\alpha_{\gamma,acute}$ estimated from mouse tumors induced by exposure to HZE and fission neutrons. The two largest values are for hepatocellular carcinomas induced by HZE in male mice. (Reproduced, with permission, from Cucinotta *et al*. 2017.)

5.3 Suggested approximation for quality factor for real-time monitoring of GCR component of exposure

When the NASA Cancer Risk Projection Model is applied to obtain REID (and its uncertainty distribution) for a specific scenario of space radiation exposure, equation (2) above is summed over the particle fluence spectrum (in terms of charge and energy of particle track segments) responsible for the dose to tissue T and over all tissues and the time of the exposure. The fluence spectra are estimated from theoretical and experimental knowledge of the relevant space radiation environment, either as prospective estimates of exposure in a future mission or as retrospective estimates for a completed mission. Real time evaluation during a mission is currently not practical due to the high demands on radiation monitoring procedures that would be required for computation of QF_{NASA} in NSCR-2012. For space exploration, the mass, volume, bandwidth and power consumption of dosimetry systems and particle spectrometers are highly constrained. Therefore, it has been suggested that a real-time dose-averaged quality factor for GCR can be estimated by use of an alternative simplified formulation of quality factor based only on the LET of the particles (Borak *et al*. 2014). The proposed approximation was developed after extensive simulations using GCR distributions in free space, as well as the resulting spectra of primary and secondary particles behind aluminium shields and penetration through water. In all cases simulated, the revised dose-averaged quality factors agreed well (within 5%) with those based on the corresponding values obtained using QF_{NASA} (Borak *et al*. 2014).

The proposal preserves the functional form of QF_{NASA} but replaces Z^{*2}/β^2 in equations (3) and (4) with LET in units of keV μm^{-1}, as follows:

$$Q_N(LET) = [1 - P(LET)] + (\Sigma_L/LET) \, . \, P(LET) \qquad (8)$$

$$\text{where} \quad P(LET) = (1 - e^{-LET/\Lambda})^m \qquad (9)$$

The new model parameters were assigned the values shown in Table 3.

Table 3. Model parameter values for proposed quality factor, Q_N, for real-time monitoring

Parameter	Solid Cancer	Leukemia
m	3.0	3.5
Λ, keV μm^{-1}	70	71
Σ_L, keV μm^{-1}	5700	1800

Borak *et al.* (2014) have shown that the shape of the resulting single-valued function of $Q_N(LET)$ versus LET is similar to the major general features of the family of curves of Q_{NASA} versus LET for particles of individual charge, but the Q_N curve has a smaller peak value at a fixed value of LET for all particles and a broader width compared to Q_{NASA} for individual values of charge.

When presenting the above suggestion for real-time monitoring, no attempt was made to assign uncertainty estimates to the individual parameter values or to the overall value of Q_N (Borak *et al*. 2014). Hence, the present suggestion does not provide for evaluation of uncertainty distributions for the real-time contribution of the GCR exposure to REID. Additionally, the contribution from SPE is not considered in this approach even though SPE can be a major source of time-varying exposure during a mission.

6. Radiation quality uncertainties not included in the cancer risk model

There remain issues related to track structure and radiation quality that are not considered at all in the quality factors as developed above.

The quality factor as defined by equations (3) or (7) for application in the cancer risk projection models NSCR-2012 or NSCR-2014, respectively, are formulated to take into account the increased effectiveness of HZE relative to reference γ-rays on the underlying assumption that the carcinogenic processes differ only quantitatively between the radiations. However, the dramatically different spatial and temporal distributions in cells and tissue of the radiation interactions from HZE tracks compared to γ-rays, leaves ample scope also for *qualitative* differences in the biological responses. In particular, there is some evidence for decreased latency and greater lethality of tumors induced by HZE particles. This issue was recognised and discussed when the NASA cancer risk projection model was formulated, but it could not be included in the model because of lack of sufficient data for its evaluation (Cucinotta *et al*. 2013). However, some estimates of the possible increased risks have been made (Cucinotta *et al*. 2015).

The risk models NSCR-2012 and NSCR-2014 are implicitly largely based on the assumptions of the conventional 'targeted' paradigm of radiobiology (Goodhead 2010). In particular, they do not include any possible modifications of risk at low doses by non-targeted "bystander" effects. Due to the low fluence rates (low dose rates) of exposure to HZE in space and the large amounts of energy deposition along each particle track, cells or regions of tissue are mostly exposed to single tracks, isolated in space and time, but each delivering a substantial dose to those cells that are directly traversed, as well as a much smaller dose to a larger number of additional cells within range of the delta-ray electrons (Curtis 2013). Most cells in the body do not experience a direct traversal by an HZE particle over quite extended periods in space travel (Curtis 2016). These circumstances of exposure to low fluence rates of high-LET particles may be optimal for expression of non-targeted effects, whereby biochemical damage signals from the traversed cells can induce effects in non-traversed cells {Morgan and Sowa 2009; Domogauer and Azzam 2014). There is some evidence, including from analyses of the shapes of dose-response in the mouse Harderian tumor data, that tumor induction at low doses (low fluences) of HZE particles may be enhanced by non-targeted effects; this mechanism could potentially increase space radiation risks by up to about 2-fold (Cucinotta and Cacao 2017).

7. Non-cancer health risks

The role of track structure in relation to other health risks from space radiation is much less well understood than it is for cancer induction. In order to specify dose limits to control non-cancer effects to the eye lens, skin, blood-forming organs and circulatory system, the NASA Space-Permissible Exposure Limits (SPELS) use a Gray Equivalent quantity, based on RBEs specified as 2.5 (range 1-4) for all heavy ions except for protons of > 2 MeV (RBE 1.5). For central nervous system non-cancer (CNS) effects the RBE is largely unknown, so a physical dose limit in mGy is specified, with a lower limit being set for particles with charge $Z \geq 10$ (NASA 2015).

The role of track structure is particularly intriguing in relation to potential effects on CNS because of the large local energy deposition along the path of an HZE particle, the high ionization

density within the particle track and the substantial lateral extension of the track by delta-ray electrons, such that the track might overlap, for example, with much of the volume of one or more neurons and interact simultaneously with many components. Monte-Carlo track structure simulations have been applied recently to gain insights into the types of initial damage that may occur to neuron cell structures from HZE particle tracks (Alp *et al*. 2015; 2017).

Acknowledgements

The author thanks Francis A. Cucinotta for helpful discussions and approval for use of diagrams and Mark R. Shavers for helpful discussions and suggestions. Opinions expressed in this article are the responsibility of the author alone, based on his judgement from the published scientific literature.

References

Alloni, D., Mariotti, L.G. and Ottolenghi, A. (2014). Early events leading to radiation-induced biological effects. In: Comprehensive Biomedical Physics. Ed. A. Brahme. Elsevier, Amsterdam; vol. 7, pp. 1-22.

Alp, M., Prihar, V.K., Limoli, C.L. and Cucinotta, F.A.. (2015). Irradiation of neurons with high-energy charged carticles: An *in silico* modeling approach. PLoS Comput. Biol. 11(8): e1004428.

Alp, M. and Cucinotta, F.A. (2017). Track structure model of microscopic energy deposition by protons and heavy ions in segments of neuronal cell dendrites represented by cylinders or spheres. Life Sc. Space Re.s 13, 27-38.

Borak, T.B., Heilbronn, L.H., Townsend, L.W. and McBeth, R.A. (2014). Quality factors for space research: A new approach. Life Sc. Sp. Res. 1, 96-102.

Cacao, E., Hada, M., Saganti, P.M., George, A. and Cucinotta, F.A. (2016). Relative biological effectiveness of HZE particles for chromosomal exchanges and other surrogate cancer risk endpoints. PLoS One 11(4): e0153998.

Chang, P.T., Cucinotta, F.A., Bjornstad, K.A., Bakke, M., Rosen, C.J., Du N, Fairchild, D.G., Cacao, E. and Blakely, E.A. (2016). Harderian gland tumorigenesis: Low-dose and LET response. Radiat. Res. 185, 449–460.

Chylack, L.T. Jr, Peterson, L.E., Feiveson, A.H., Wear, M.L., Manuel, F.K., Tung, W.H., Hardy, D.S., Marak, L.J. and Cucinotta, F.A. (2009). NASA study of cataract in astronauts (NASCA). Report 1: Cross-sectional study of the relationship of exposure to space radiation and risk of lens opacity. Radiat. Res. 172, 10-20.

Cucinotta, F.A. (2015a) Review of NASA approach to space radiation risk assessments for Mars exploration. Health Physics 108, 131–42.

Cucinotta, F.A. (2015b). A new approach to reduce uncertainties in space radiation cancer risk predictions. PloS One 2015; 10e0120717.

Cucinotta, F.A. and Cacao, E. (2017). Non-targeted effects models predict significantly higher Mars mission cancer risk than targeted effects models. Scientific Reports 7:1832, 1-11.

Cucinotta, F,A,, Kim, M.Y. and Chappell L. (2013). Space radiation cancer risk projections and uncertainties - 2012; NASA Report no. NASA/TP-2013-217375. Houston: National Aeronautics and Space Administration.

Cucinotta, F.A., Alp, M., Rowedder, B. and Kim, M.Y. (2015) Safe days in space with acceptable uncertainty from space radiation exposure. Life Sc. Space Res. 5, 31–38.

Cucinotta, F.A., Cacao, E. and Alp, M. (2016). Space radiation quality factors and the delta ray dose and dose-rate reduction effectiveness factor. Health Phys 110, 262–6.

Cucinotta, F.A., To, K. and Cacao, E. (2017). Predictions of space radiation fatality risk for exploration missions. Life Sc.Space Res. 13, 1–11.

Curtis, S.B. (2013). Fluence rates, delta rays and cell nucleus hit rates from galactic cosmic rays. https://three.jsc.nasa.gov/articles/TracksinSpace.pdf. Date posted: 02-28-2013.

Curtis, S.B. (2016). Introduction to track structure and Z^{*2}/β^2. https://three.jsc.nasa.gov/articles/Track-Structure-SCurtis.pdf. Date posted: 02-29-2016.

Domogauer, J. and Azzam, E.I. (2014). The radiation response in cells not directly traversed by high charge and high energy particles: The bystander effect of space radiation. https://three.jsc.nasa.gov/articles/Azzams-Bystander-Effect.pdf. Date posted 03-10-14.

Goodhead, D.T. (1988). Spatial and temporal distribution of energy. Health Physics 55, 231-240.

Goodhead, D.T. (1994). Initial events in the cellular effects of ionizing radiations: clustered damage in DNA. Int. J Radiat. Biol. 65, 7-17.

Goodhead, D.T. (2009). Fifth Warren K. Sinclair keynote address: Issues in quantifying the effects of low-level radiation. Health Physics. 97, 394-406.

Goodhead, D.T. (2010). New radiobiological, radiation risk and radiation protection paradigms. Mutat. Res. 687, 13-16.

ICRP (103) (2007). The 2007 Recommendations of the International Commission on Radiological Protection. Annals of the ICRP, Publication 103. The International Commission on Radiological Protection.

Katz, R., Ackerson B., Homayoonfar, M. and Sharma, S.C. (1971). Inactivation of cells by heavy ion bombardment. Radiat. Res. 47, 402–425.

Morgan, W.F. and Sowa, M.B. (2009). Non-targeted effects of ionizing radiation: Implications for risk assessment and the radiation dose response profile. Health Physics 97, 426-432.

NA/NRC (2012). Technical evaluation of the NASA model for cancer risk to astronauts due to space radiation. National Academies/National Research Council. Washington, DC: National Academies Press.

NASA (2015). NASA Space Flight Human-System Standard, Vol 1, Revision A: Crew Health, National Aeronautics and Space Administration, NASA-STD-3001, Vol 1, Revision A w/Change 1.

NCRP (2014). Radiation Protection for Space Activities: Supplement to Previous Recommendations. NCRP Commentary 23. National Council on Radiation Protection and Measurements, Bethesda.

NCRP (2018) Evaluation of the relative effectiveness of low-energy photons and electrons in inducing cancer in humans. NCRP Report (in press). National Council on Radiation Protection and Measurements (Bethesda, MD).

Plante, I. and Cucinotta, F.A. (2008). Ionization and excitation cross sections for the interaction of HZE particles in liquid water and application to Monte-Carlo simulation of radiation tracks. New J of Phys. 10:125020, 1-15.

Schimmerling, W. (2011). The space radiation environment: an introduction. https://three.jsc.nasa.gov/concepts/SpaceRadiationEnviron.pdf. Date posted: 02-05-2011.

Suman, S., Kumar, S., Moon, B.H., Strawn, S.J., Thakor, H., Fan, Z., Shay, J.W., Fornace Jr, A.J. and Datta, K., (2016). Relative biological effectiveness of energetic heavy ions for intestinal tumorigenesis shows male preponderance and radiation type and energy dependence in APC 1638N/ + mice. Int. J. Radiat. Oncol. Biol. Phys. 95, 131–138.

Toburen, L. (2014). Development of Monte Carlo track structure codes. https://three.jsc.nasa.gov/articles/Monte-Carlo-Track-Structure-Toburen.pdf. Date posted: 02-06-2014.